Journal of Optoelectronic and Biomedical Materials Vol. 16, No. 4, October–December 2024, p. 221-228

SnO_2 nanoparticle synthesis using coriandrum sativum plant extract: evaluation of antibacterial and antifungal activity

M. A. Obaid [a,*], K. A. Hussein [b], S. A. Khlaf [c]

[a].*Department of Medical Physics, College of Applied Medical Science, Shatrah University, Thi-Qar, 64001, Iraq*

[b] *Pharmaceutical Department, College of Pharmacy, University of Thi-Qar, Iraq*

[c] *Ministry of Education, Al-Karkh 3, Al-Fatemiyyat Preparatory, Iraq*

This paper presents a method for synthesizing SnO2 nanoparticles in an environmentally benign manner. The nanoparticles are then subjected to analysis to evaluate their structural, optical, morphological, and anti-bacterial properties. The analysis is conducted using an extract derived from Coriandrum sativum. XRD FTIR, UV-Vis, AFM, and SEM studies were used to evaluate the synthesized SnO2 nanoparticles. SnO2 was found to be present in the rutile phase based on X-ray diffraction (XRD) examination. The phase had a tetragonal structure and a crystalline size of 70.83 nm. SnO2 nanoparticles' FTIR spectra show a distinctive Sn–O–Sn bond vibration band, which spans a frequency range of 580 to 729 (1/cm). The SnO2 sample demonstrates favorable transmission within the wavelength range of approximately 400 nm to 1100 nm, with a maximum transmittance of 96% at 1100 nm. The SnO2 nanoparticles possess a direct band gap with a magnitude of 4.51 electron volts (eV). The root mean square (RMS) roughness was measured to be 2.06129 nm, both overall and on a grain-wise basis, using atomic force microscopy (AFM). Additionally, the mean roughness (Sa) was found to be 1.67382 nm. The SEM investigation indicated that the SnO2 particles had a semispherical shape and formed aggregates like flowers, with protruding hemispherical ends. The grains exhibited a range of main axis diameters, varying from 0.01 to 0.16 µm, with an average size of 0.1 µm. In addition, SnO2 nanoparticles were utilized as antimicrobials, efficiently interacting with cell membranes to deactivate bacteria and fungi.

(Received September 21, 2024; Accepted December 23, 2024)

Keywords: Coriandrum sativum, SnO2 surface morphology, FTIR analysis, Crystalline size, ZOI

1. Introduction

Nanomaterials and Nano science, a field that combines advanced technologies from several disciplines such as “physics, chemistry, biology, material science, and medicine”, has become a prominent topic of research in recent times. Eliminating dangerous compounds was essential, and most of the techniques used to achieve efficient manufacture of environmentally friendly nanoparticles were environmentally friendly technologies [1–5]. Scientists from many disciplines such as biology, chemistry, materials science of materials, and the pursuit of eco-friendly methods for creating inorganic materials, are highly interested in green synthesis [7-9]. Transition metal nanoparticles are increasingly significant due to their ability to be manufactured by plants, as well as their low toxicity, bio-compatibility, environmentally benign nature, and green approach. SnO2 nanoparticles exhibit properties of a p-type semiconductor metal and possess a direct optical band gap energy ranging from 2.5 to 3.4 eV. SnO2 nanoparticles have been produced using several methods such as spray pyrolysis, hydrothermal, co-precipitation, and microwave-assisted procedures [10–12]. Nevertheless, green nanoparticle synthesis is attracting more interest as compared to the procedures mentioned above. The main reason for the increasing importance of the green approach to creating nano metal oxides is its cost-effectiveness, capacity to generate high-yield nanoparticles, and other benefits compared to alternative methods [13, 14]. Due to the limited research on the use of plant extracts as capping and reducing agents for the green synthesis of SnO2,

* Corresponding author: hamedalwan14@gmail.com
https://doi.org/10.15251/JOBM.2024.164.221

we opted to apply a secondary metabolite-mediated approach to produce SnO2 nanoparticles. It is worth noting that these nanoparticles often have an amorphous structure rather than a crystalline one [10]. The SnO2 nanoparticle exhibits several morphologies, such as hollow spheres, meso-porous structures, nano-wires, nano-belts, and nanotubes [11]. The aim of this study is to decrease the amount of tin chloride and convert it into tin oxide nanoparticles. This will be achieved by utilizing a biomaterial that meets two primary requirements: it should be produced quickly and inexpensively, and it should be environmentally safe, without generating any harmful industrial waste. We present a cost-efficient and straightforward method for synthesizing SnO2 nanoparticles utilizing an extract obtained from Coriandrum sativum, which serves as both a capping and reducing agent. Coriander, an aromatic herb with potent fragrance and many antioxidants, is a member of the Apiaceae family. The plant is a perennial herbaceous species commonly employed in culinary practices due to its annual growth cycle and numerous medicinal properties. It possesses the capacity to enhance the health of the cardiovascular, neurological, cutaneous, and gastrointestinal systems, as well as assist in lowering blood sugar levels and fighting infections [14]. Synthetic SnO2 nanoparticles have undergone testing on both gram-positive bacteria and fungus.

Fig. 1. C.s. plant.

2. Preparation of SnO2 suspension

The Coriandrum sativum (C.s.) plant bought from (Iraq/Baghdad) market in Iraq. Deionized water, often known as DI water, was utilized for the purpose of washing. The C.s.plant was rinsed and subsequently air-dried for a duration of 48 hours at ambient temperature. The dried plant material was pulverized into a fine powder using a domestic mixer, commonly known as a mixer. The powdered plant, weighing two grams, was subsequently combined with one hundred milliliters of deionized water and transferred into an Erlenmeyer flask. The dispersion underwent heating at a temperature of 60 °C for 30 minutes. After the extract from the C.s.plant has cooled to the temperature of the surrounding room, it is passed through a filter paper known as Whatman No. 1 to remove impurities. The manufacture of SnO2 nanoparticles began by mixing 100 mL of water with 1.8 g of SnCl2 (0.1 M) precursor. After adding 20 mL of C.s.extract to the previous mixture, it was stirred for 60 minutes at a temperature of 70 degrees Celsius. Figure 2 depicts a powdered C.s.and solution of SnO2.

Fig. 2. Dry C.s. plant powder and SnO2 solution.

3. Results and discussion

Figure 3 depicts (XRD) patterns of the SnO2 thin film synthesized using the C.s. plant extract. By employing this characterization technique, we can deduce that the material consists of tin oxide with a high degree of structural purity. The dominant peaks in the X-ray diffraction pattern occur at 2θ values of 26.68° and 33.94°, which can be attributed to the crystal planes (110) and (101) respectively. This material lacks any additional crystalline phases that do not align with those of SnO2. According to "JCPDS file No. 41-1445" [15–17], the evidence indicates that SnO2 adopts a tetragonal structure during the rutile phase. SnO2 crystals have a diameter of 70.83 nanometers.

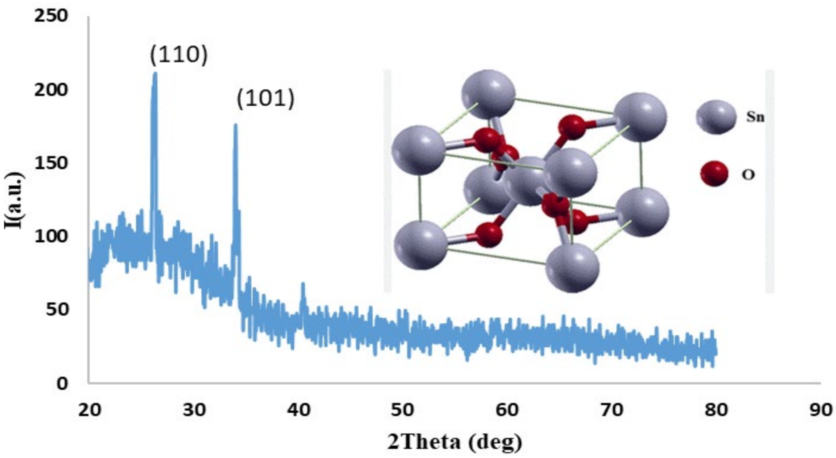

Fig. 3. Structural properties of SnO film by XRD.

Figure 4 depicts the range of 4000–450 (1/cm) in which the (FTIR) spectra of the SnO2 NPs were measured using an FTIR spectro-photometer (PerkinElmer / USA). The infrared spectra indicate that the leaf extract contains O-H groups, which are located in the band area at 3410 (1/cm). The peak area at 2923 (1/cm) is indicative of the vibrational C-H ring stretching. A stretching vibration at 1631 (1/cm) indicates the existence of carbonyl (C=O) groups. The FTIR spectra exhibit the characteristic vibrations of the Sn-O-Sn bond, which occur within the range of 580 to 729 (1/cm) [18–21].

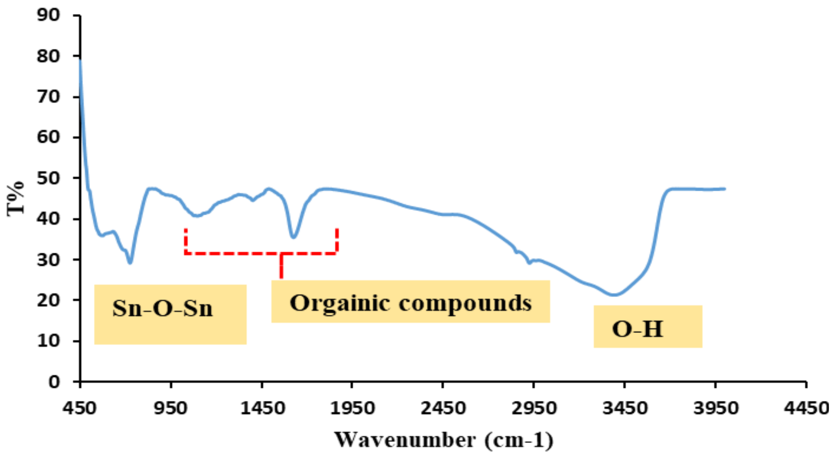

Fig. 4. FTIR analyses of SnO NPs.

A helpful, non-destructive method for analyzing the optical characteristics of semiconducting nanoparticles is UV-visible absorption spectroscopy. It is anticipated that a wide range of variables may affect absorbance, including oxygen deprivation, surface roughness, band gap, and impurity centers. Because of the small particle size, which can be thought of as a blue-shift of the optical absorption edge due to band gap expansion in the UV region, quantum confinement effects are predicted. As illustrated in Fig. 5a, the UV–Vis spectra of the SnO2 NPs display the transmittance spectrum as a function of wavelength in the range of 190–1100 nm. According to the discovered transmission spectrum, there is a high transmission between 400 and 1100 nm in wavelength. According to the spectra, there is a noticeable absorption in the wavelength range of 190 to 300 nm, and at 1100 nm, there is the highest transmittance of 96%. To find the band gap, apply the formula $[(\alpha h\nu) = B(h\nu - Eg)^n]$. The incident photon energy is represented by hν, the band tailing parameter is a constant, and the value for the direct transition is n. The direct band gap was calculated using a Tauc plot, which is drawn between hν and the $(\alpha h\nu)^2$. Figure 5b shows the band gap of SnO2 nanoparticles. The straight band gap of SnO2 nanoparticles is 4.51 eV. The band gap of SnO2 nanoparticles is larger than that of their bulk equivalent due to the quantum confinement effect [20–24]. It is possible that additional variables, such as lattice strain, could impact the nanoparticle' energy levels. Based on the samples' band gap, biogenic tin oxide appears to be a good option for optical applications.

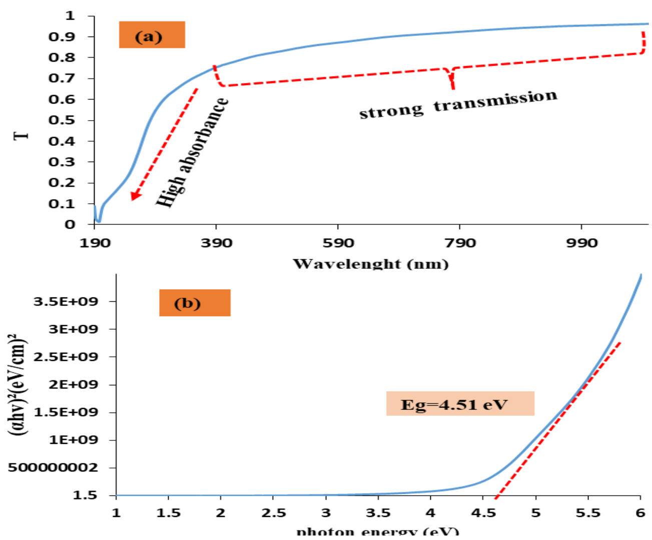

Fig. 5. (a) Transmission spectra of SnO2 nanoparticles (b) Tauc's plot to determine the energy gap.

A study was conducted to analyze the surface topography of SnO2 thin films generated using the spin coating technique. Atomic force microscopy (AFM) was used to examine a 2 × 2 µm area as shown in figure6. The measurements yielded a mean roughness (Sa) of 1.67382 nm, an RMS roughness (Sq) of 2.06129 nm, and an RMS roughness (grain-wise) of 2.06129 nm.

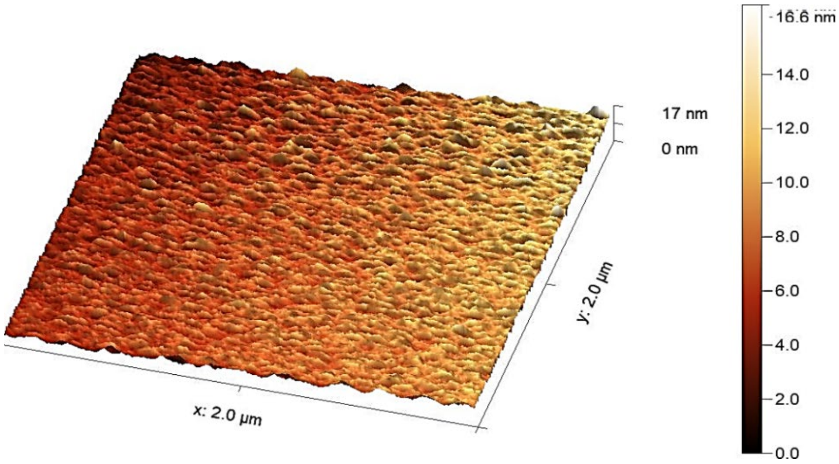

Fig. 6. Topography properties of SnO film by AFM.

The physical composition of a thin layer of SnO2 created by spin coating is shown in Figure 7, which was obtained after 10 or 15 minutes at 80C. An eco-friendly technique was used to create the thin film. The semispherical, flower-like aggregates and SnO2 spheres with protruding hemispherical ends are shown in detail in Figure 6. The grains have an average size of 0.1 µm and vary in size from 0.01 to 0.16 µm along their principal axis.

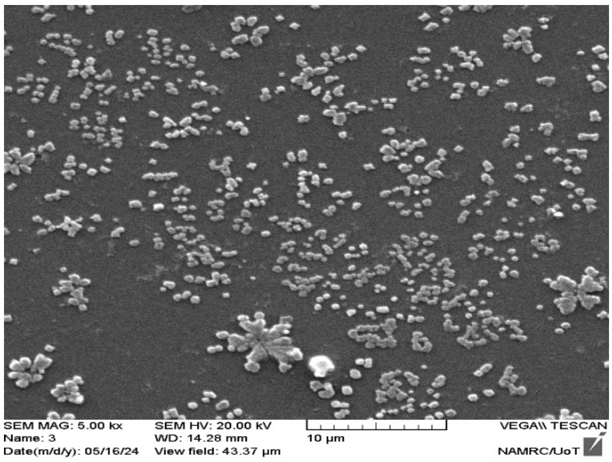

Fig. 7. Morphology properties of SnO film by SEM.

The anti-bacterial activities of SnO2 NPs were assessed against clinically isolated instances of "Gram-positive, Gram-negative", and fungal infections using the Agar well diffusion method. The SnO2 nano-particles are evenly distributed inside the media and interact with it in a plate that has been inoculated with the test organisms. Figure 8 and Table 1 demonstrate that the resulting zones of inhibition will consistently exhibit a circular shape, with a diameter measured in millimeters [25-27]. The experiment illustrates the substantial inhibitory effect of SnO2 NPs on bacterial culture growth. A bacterium with a complicated cell wall structure and a negative Gram stain result. The cell wall of the organism consists of an outer membrane that envelops the surface membrane and a substantial layer. The complex structure of this cell wall reduces its efficiency. Metal oxide nanoparticles exhibit enhanced chemical and biological activity due to their substantial surface area. The bacterial cell membrane interacts with the reactive oxygen species produced by the presence of SnO2 NPs, which enables the nanoparticles to enter the cell. Figure 9 presents a schematic representation that depicts a possible mechanism of anti-bacterial activity. The interaction between SnO2 NPs and the cell membrane is highly effective due to their specific features, leading to the inactivation of bacteria. Metal oxide nanoparticles exhibit anti-bacterial properties through multiple mechanisms, including as photocatalytic activation by light, electrostatic interaction with cell walls, and particle degradation leading to the generation of reactive oxygen species. Nanostructures can interact with bacterial cells using these techniques, resulting in the formation of a zone of inhibition (ZOI) around nano-materials. The (ZOI) is determined by the bactericidal efficiency of nanoparticles. (ZOI) surrounding SnO2 NPs is smaller when compared to the positive control. In order to improve ZOI, it is necessary to do more comprehensive research on adjusting the surface or modifying the reaction parameters and manufacturing method of the nanoparticles [28-30].

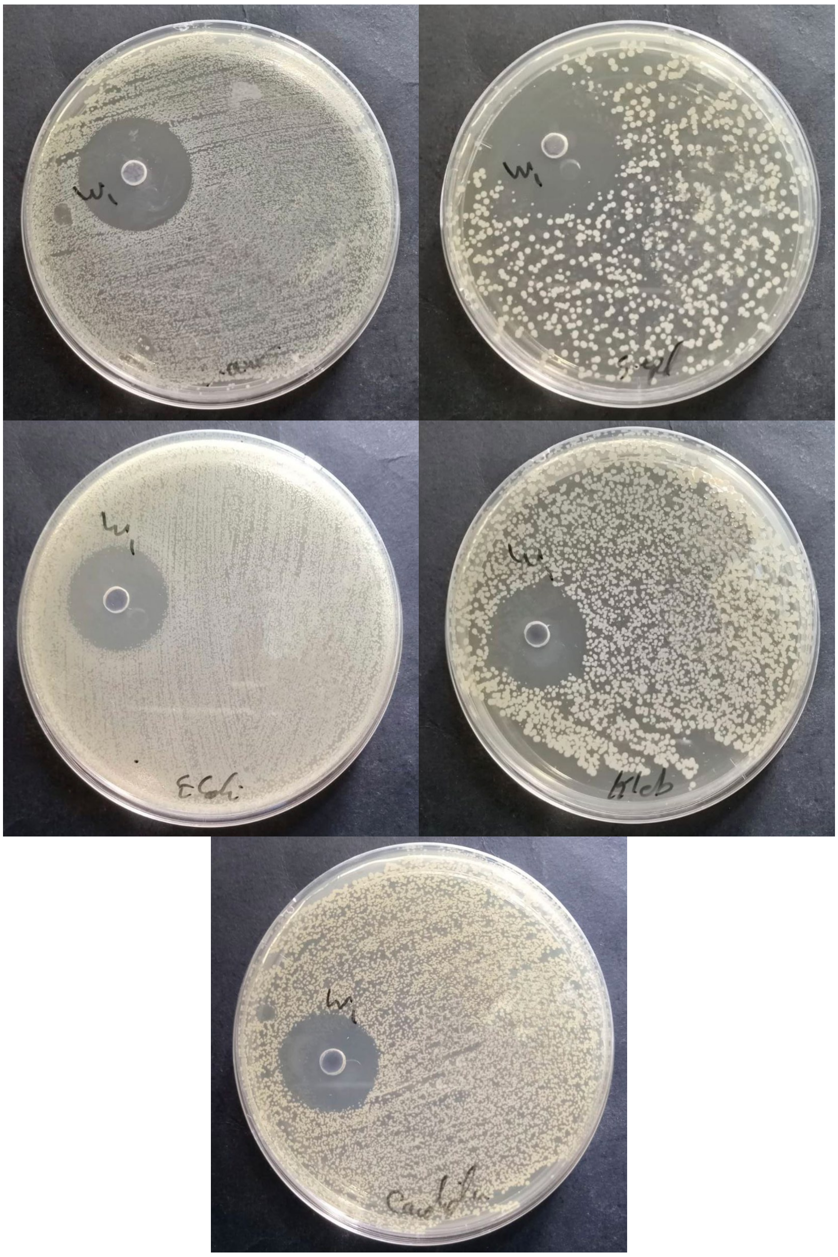

Fig. 8. Inhibition region of G+ve, inhibition region of G-ve and stain fungi.

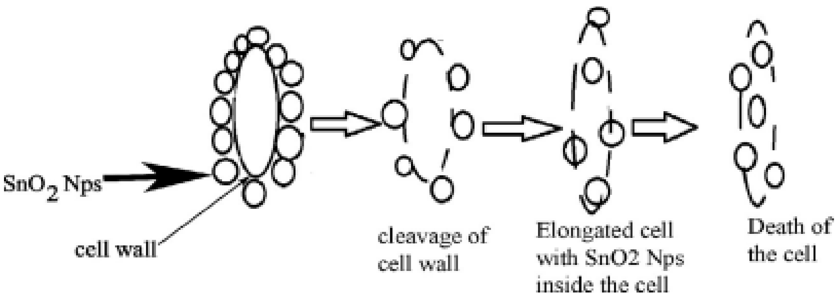

Fig. 9. Schematic diagram showing possible mechanism of anti-bacterial activity.

Table 1. Results of inhibition zone.

Gram Positive bactrial		Gram negative bactrial		fungal
Staphylococcus aureus Staphylococcus epid.	27 mm 33 mm	**E-coli** **Klebsiella sp.**	**23 mm** **23 mm**	**Candida 22 mm**

4. Conclusion

The synthesis of SnO2 NPs was achieved using innovative and environmentally friendly methods, utilizing C.s. extract as a reducing agent. Our conclusion is that SnO2 transparent materials cannot absorb photons with energy values below their band gap value. As a result, they enable visible light to flow through. The findings suggest that SnO2 NPs can serve as an oxidation catalyst due to their possession of multivalent oxidation states, enabling them to readily release lattice oxygen to react with adsorbed molecules. Additionally, these nanoparticles can function as a window layer in solar cells, as they exhibit high transmission spectra beyond 390 nm wavelengths. Our study paper is pioneering in its utilization of coriander for the synthesis of tin oxide, and its impact on microorganisms was demonstrated through the measurement of inhibitory zone diameters.

References

[1] Ganesh Elango, Subramanian Manoj Kumaran, Sekar anthosh Kumar, Soundrapandian Muthuraja, Spectrochimica Acta Part A: Molecular and Biomolecular Spectroscopy vol 145, (2015), 176-180; https://doi.org/10.1016/j.saa.2015.03.033

[2] Mayedwa N, Mongwaketsi N, Khamlich S, Kaviyarasu K, Matinise N, Maaza M Green Appl Surf Sci 446, (2018) 250-257; https://doi.org/10.1016/j.apsusc.2017.12.161

[3] Magdalane CM, Kaviyarasu K, Priyadharsini GMA, Bashir AKH, Mayedwa N, Matinise N, Isaev AB, Al-Dhabi NA, Mariadhas ValanArasu M, Arokiyaraj S, Kennedy J, Maaza M J Mater Res Techno; 8(3) (2019),2898-2909; https://doi.org/10.1016/j.jmrt.2018.11.019

[4]. Hui-Chi C, Chen-Sheng Y, J Phys Chem C 111(2007) 7256-7259; https://doi.org/10.1021/jp0688355

[5] Guanglu S, Jihuai W, Miaoliang H, Jianming L, Zhang L, Yunfang H, Fan L J Phys Chem C 116(2012)20140-20145; https://doi.org/10.1021/jp304185q

[6] Taebaraek Safaa Attaa, Ahmed Naji Abd , Muayyed Jabar Zoory Materials Today: Proceedings 49 (2022) 3607-3614; https://doi.org/10.1016/j.matpr.2021.08.152

[7] H.A. Naif, A. M. Abbas, M. F. H.Al-Kadhemy: Investigate Spectroscopic Experimental and Theoretical Model for Hemoglobin Nanoscale Solution. Baghdad Sci.J. 21 (2) 2024 :465-472; https://doi.org/10.21123/bsj.2023.7775

[8] Taebaraek Safaa Attaa , Ahmed Naji Abd , Muayyed Jabar Zoory , Journal of Physics: Conference Series 1963 (2021) 012148 ,IOP Publishing; https://doi.org/10.1088/1742-6596/1963/1/012148
[9] Hamed A. Gatea, The European Physical Journal D, Vol. 76, no. 148,(2022).
[10] Arularasu MV, Anbarasu M, Poovaragan S, Sundaram R, Kanimozhi K, Maaza M J Nanosci Nanotechnol 18(5) (2018) 3511-3517; https://doi.org/10.1166/jnn.2018.14658
[11] AMM Hamed. A. Gatea, Maithm. A. Obaid, Degest Journal of Nanomaterials and Biostrctures 19 (3), 1117-1127,2024; https://doi.org/10.15251/DJNB.2024.193.1117
[12] Suresh KC, Sudha M, Balamurugan A, Surendhiran S, Manojkumar P, Syed Khadar YA J Inf Comput Sci 9(12) (2019) 401-413
[13] Sudha M, Balamurugan A, Surendhiran S, Manojkumar P, Syed Khadar YA J Inf Comput Sci 9(12) (2019) 396-406
[14] Alessandra Carrubba, J Sci Food Agric, 89(2009) 921-926; https://doi.org/10.1002/jsfa.3535
[15] D. Singh, V.S. Kundu, A.S. MaanJ. Mol. Struct. (2016)1115, 250; https://doi.org/10.1016/j.molstruc.2016.02.091
[16] P. Amornpitoksuk, S. Suwanboon, S. Kaowphong, Sustain. Chem. Pharm. 14, (2019); https://doi.org/10.1016/j.scp.2019.100190
[17] S. Sathishkumar, M. Parthibavarman, V. Sharmila, M. Karthik, J. Mater. Sci. Mater. Electron. 28, (2017)8192; https://doi.org/10.1007/s10854-017-6529-y
[18] K. C. Suresh, S. Surendhiran, P. Manoj Kumar, E. Ranjth Kumar, Y. A. Syed Khadar, A. Balamurugan, SN Applied Sciences 2 (2020) 1735; https://doi.org/10.1007/s42452-020-03534-z
[19] S. Bhavana, Vinod Gubbiveeranna, C. G. Kusuma, H. Ravikumar, C. K. Sumachirayu, H. Nagabhushana & S. Nagaraju30,(2019)431-437; https://doi.org/10.1007/s10876-019-01496-w
[20] Hamed A. Gatea, Nanoscience & Nanotechnology-Asia 11 (3), 322-329, 2021; https://doi.org/10.2174/2210681210999200715105250
[21] J. Gajendiran, V. Rajendran, Mater. Lett. 139, (2015)116; https://doi.org/10.1016/j.matlet.2014.10.056
[22] P. A. Luque, O. Nava, C. A. Soto Robles, H. E. Garrafa Galvez, M. E. Martínez Rosas, M. J. Chinchillas Chinchillas, A. R. Vilchis Nestor, A. Castro Beltrán, Journal of Materials Science: Materials in Electronics (2020); https://doi.org/10.1007/s10854-020-04242-5
[23] V.K. Vidhu, Daizy Philip Spectrochimica Acta Part A: Molecular and Biomolecular Spectroscopy 134 (2015) 372-379; https://doi.org/10.1016/j.saa.2014.06.131
[24] Periathai RS, Pandiyarajan J, Jeyakumaran N, Prithivikumaran N IJCRGG 3(2014)2132-2134
[25] Hamed A. Gatea, International Journal of Thin Films Science and Technology 11 (2), 201,2022.
[26] Salih, A.A., Abad, W.K., Fadaam, S.A., Hussein, B.H. Digest Journal of Nanomaterials and Biostructures; 18(4)(2023). 1225-1233; https://doi.org/10.15251/DJNB.2023.184.1225
[27] S.H. Chaki, M.P. Deshpande, J.P. Tailor, Thin Solid Films 550 (2014) 291-297; https://doi.org/10.1016/j.tsf.2013.11.037
[28] Abad, W.K., Abd, A.N., Habubi, N.F. Nano Biomedicine and EngineeringThis link is disabled., 15(4)(2023), pp. 363-368; https://doi.org/10.26599/NBE.2023.9290032
[29] Véronique B. Schwartz, Franck Thétiot, Sandra Ritz, Sabine Pütz, Lars Choritz, Adv. Funct. Mater., 22, (2012)2376-2386; https://doi.org/10.1002/adfm.201102980
[30] Nancy John, Malu Somaraj, Nisha, J IOP Conf. Series: Materials Science and Engineering 360 (2018) 012007; https://doi.org/10.1088/1757-899X/360/1/012007